

AD-A111 309

ADMIRALTY MARINE TECHNOLOGY ESTABLISHMENT TEDDINGTON--ETC F/6 20/4
FREE-WAVE PROPAGATION IN FLUID-LOADED THICK-WALLED CIRCULAR PIP--ETC(U)
NOV 81 S A LESTER

UNCLASSIFIED AMTE(N)-TM81093

DRIC-BR-81307

NL

1 OF 1
AD-A
111 309

END
DATE
FILMED
10-82
DTIC

AD A11 1309

ANTE (N) 1309

OLD COPY

NAVY
MARINE TECHNOLOGY
ESTABLISHMENT

FREE-WAVE PROPAGATION IN FLUID-LOADED
THICK-WALLED CIRCULAR PIPES

S. A. LESTER

DTIC
ELECTE
FEB 23 1982

FREE-WAVE PROPAGATION IN FLUID-LOADED
THICK-WALLED CIRCULAR PIPES

BY

S A LESTER

Summary

An infinite thick-walled pipe contains, and is surrounded by, an inviscid fluid. The displacements of the pipe's wall satisfy the exact linear equations of elasticity, and the interior and exterior fluids satisfy the scalar Helmholtz wave equation. The differential equations are solved by means of Fourier transforms to give the dispersion relation connecting frequency with axial and circumferential wavenumbers. The dispersion relation is solved numerically to give examples of 'real' axial wavenumber versus frequency plots for selected circumferential harmonics.

20 pages
3 figures

AMTE(Teddington)
Queen's Road
TEDDINGTON Middlesex TW11 0LN

November 1981

C

Copyright
Controller HMSO London
1981

- 1 -

Accession For	
NTIS GRA&I	X
DTIC TAB	
Unannounced	
Justification	
By	
Date	
File	
Index	
Search	
Serials	
Other	
A	

LIST OF SYMBOLS

(r, ϕ, z)	cylindrical coordinates
$u_r(r, \phi, z), u_\phi, u_z$	radial, tangential and axial displacements
$u_r(n, \alpha, r), \text{ etc}$	Fourier transforms of displacements
n, α	circumferential harmonic number, axial wavenumber
$\tau_{rr}, \tau_{r\phi}, \tau_{rz}$	stresses in pipe wall
ω	radian frequency of vibration, $= 2\pi f$
a, b	inner and outer radius of pipe wall
λ, μ	Lamé elastic constants
k_l, k_s	elastic wavenumbers, ω/c_l and ω/c_s
c_l	velocity of longitudinal wave, $= \sqrt{[(\lambda+2\mu)/\rho]}$
c_s	velocity of shear wave, $= \sqrt{(\mu/\rho)}$
γ_l	$\sqrt{(k_l^2 - \alpha^2)} \quad \text{Im}(\gamma_l) > 0$
γ_s	$\sqrt{(k_s^2 - \alpha^2)} \quad \text{Im}(\gamma_s) > 0$
$p_e(r, \phi, z), p_i(r, \phi, z)$	exterior and interior fluid pressures
ρ_e, ρ_i, c_e, c_i	fluid densities and sound velocities
k_e, k_i	fluid wavenumbers, ω/c_e and ω/c_i
γ_e	$\sqrt{(k_e^2 - \alpha^2)} \quad \text{Im}(\gamma_e) > 0$
γ_i	$\sqrt{(k_i^2 - \alpha^2)} \quad \text{Im}(\gamma_i) > 0$
J_n, J'_n, Y_n, Y'_n	Bessel functions and derivatives
H_n, H'_n	Hankel functions, $J_n + iY_n, J'_n + iY'_n$
$[M]$ i^*j	a matrix, i rows and j columns

INTRODUCTION

Interpretation of the vibration and sound radiation of fluid-filled pipes is facilitated greatly by the availability of axial wavenumber versus frequency plots. Fuller and Fahy [1] discuss the physical significance of the real and complex branches of the wavenumber-frequency plots of fluid-filled pipes. Walter [2] uses plots of the real branches to demonstrate that the maximum responses of an air-filled pipe wall occur at frequencies at which the in-vacuo pipe and rigid-walled duct mode wavenumber-frequency plots cross each other. James [3] shows that the sound radiation from fluid-filled pipes is better understood when the real branches of the wavenumber-frequency plots are available.

Each of the above authors uses a shell theory [4] to describe the pipe wall vibrations. However, much of the pipework in industrial use is thick-walled, so it is necessary to compute wavenumber-frequency plots based on exact linear elastic theory in order to check the validity of shell theory. Kumar [5] studies the real and complex wavenumber plots of fluid-filled pipes using the exact theory for axisymmetric vibrations. Gazis [9] uses exact linear theory to investigate three-dimensional free-wave propagation in hollow elastic cylinders.

Contained in this report is the mathematical analysis needed to obtain the dispersion relation of a thick-walled pipe that contains and is surrounded by a fluid. Exact linear elastic theory for an isotropic circular pipe undergoing arbitrary motion is used. The purpose of the work is twofold. First, it provides the initial stage in the analysis of wave-propagation and sound radiation by layered pipes, corresponding to previous work on layered media [6]. Secondly, it is a computational tool for studying free-wave propagation in fluid-filled thick pipes and it is particularly valuable for making comparisons with shell theory.

2. PROBLEM FORMULATION

An infinite thick-walled circular pipe contains and is surrounded by acoustic fluids of possibly different density and sound velocity. Figure 1 shows the geometry of interest. The time harmonic factor $\exp(-i\omega t)$ is omitted from all equations.

It is assumed that the displacements (u_r, u_ϕ, u_z) of the pipe are governed by the exact linear equations of elasticity. It is convenient to represent these displacements as Fourier transforms

$$\begin{bmatrix} u_r(r, \phi, z) \\ u_\phi(r, \phi, z) \\ u_z(r, \phi, z) \end{bmatrix} = (1/2\pi) \sum_{n=0}^{\infty} \begin{bmatrix} \cos(n\phi) \\ \sin(n\phi) \\ \cos(n\phi) \end{bmatrix} \int_{-\infty}^{\infty} \exp(iaz) \begin{bmatrix} u_r(n, \alpha, r) \\ u_\phi(n, \alpha, r) \\ u_z(n, \alpha, r) \end{bmatrix} d\alpha \quad (2.1)$$

with u_r and u_z having even dependence upon the circumferential coordinate ϕ and u_ϕ having odd dependence.

The equations of elasticity are coupled in terms of the variables u_r , u_ϕ and u_z , so it is desirable to express these displacements in terms of unknowns (F, G, H) which satisfy wave-equations. These functions are also represented by Fourier transforms

$$\begin{bmatrix} F(r, \phi, z) \\ G(r, \phi, z) \\ H(r, \phi, z) \end{bmatrix} = (1/2\pi) \sum_{n=0}^{\infty} \begin{bmatrix} \cos(n\phi) \\ \sin(n\phi) \\ \cos(n\phi) \end{bmatrix} \int_{-\infty}^{\infty} \exp(iaz) \begin{bmatrix} F(n, \alpha, r) \\ G(n, \alpha, r) \\ H(n, \alpha, r) \end{bmatrix} d\alpha \quad (2.2)$$

The stresses in the pipe's wall have the Fourier transforms

$$\begin{bmatrix} \tau_{rr}(r, \phi, z) \\ \tau_{r\phi}(r, \phi, z) \\ \tau_{rz}(r, \phi, z) \end{bmatrix} = (1/2\pi) \sum_{n=0}^{\infty} \begin{bmatrix} \cos(n\phi) \\ \sin(n\phi) \\ \cos(n\phi) \end{bmatrix} \int_{-\infty}^{\infty} \exp(iaz) \begin{bmatrix} \tau_{rr}(n, \alpha, r) \\ \tau_{r\phi}(n, \alpha, r) \\ \tau_{rz}(n, \alpha, r) \end{bmatrix} d\alpha \quad (2.3)$$

and the exterior and interior fluids have the transform

$$p(r, \phi, z) = (1/2\pi) \sum_{n=0}^{\infty} \cos(n\phi) \int_{-\infty}^{\infty} \exp(iaz) p(n, \alpha, r) d\alpha \quad (2.4)$$

The Fourier transform representations facilitate solution of the wave-equations and enable relations between unknowns to be presented in 'spectral' form. The variable α is the axial wavenumber, and n is the number of wavelengths around the circumference.

The procedure for solution is as follows. First, matrix relations between the surface spectral stresses and displacements are obtained, Section 3. Secondly, the spectral pressures due to the interior and exterior fluids are expressed in terms of the spectral displacements of the inner and outer surface respectively, Section 4. Finally, the pipe-fluid boundary conditions are applied and the conditions necessary for free-wave propagation are established, Section 5.

3. THE ELASTIC LAYER

Figure 1 shows a section through a pipe whose inner boundary is $r=a$ and whose outer boundary is $r=b$. The surfaces are subject to prescribed normal and tangential spectral stresses

$$[\tau(n, \alpha)] = [\tau_{rr}^b, \tau_{r\phi}^b, \tau_{rz}^b, \tau_{rr}^a, \tau_{r\phi}^a, \tau_{rz}^a]^T \quad (3.1)$$

which produce spectral surface displacements

$$[u(n, \alpha)] = [u_r^b, u_\phi^b, u_z^b, u_r^a, u_\phi^a, u_z^a]^T \quad (3.2)$$

A relation is required between the surface spectral stresses and displacements.

The linear elastic equations of motion [7]

$$(\lambda + \mu) \text{grad}(\text{div } \underline{u}) + \mu \nabla^2 \underline{u} = \rho \partial^2 \underline{u} / \partial t^2 \quad (3.3)$$

are reduced to three wave equations

$$\nabla^2 F + k_1^2 F = 0, \quad \nabla^2 G + k_s^2 G = 0, \quad \nabla^2 H + k_s^2 H = 0 \quad (3.4)$$

by means of the substitutions

$$\begin{aligned} u_r &= \partial F / \partial r + (1/r) \partial G / \partial \phi - \partial^2 H / \partial r \partial z \\ u_\phi &= (1/r) \partial F / \partial \phi - \partial G / \partial r - (1/r) \partial^2 H / \partial \phi \partial z \\ u_z &= \partial F / \partial z + \partial^2 H / \partial r^2 + (1/r) \partial H / \partial r + (1/r^2) \partial^2 H / \partial \phi^2 = \partial F / \partial z + \nabla^2 H - \partial^2 H / \partial z^2 \end{aligned} \quad (3.5)$$

Substituting the Fourier transform representations of F, G and H into the equations (3.4) gives, after integrating the resulting equations, the spectral equations

$$\begin{aligned} F(n, \alpha, r) &= J_n(\gamma_1 r) A_1 + Y_n(\gamma_1 r) A_2 \\ G(n, \alpha, r) &= J_n(\gamma_s r) A_3 + Y_n(\gamma_s r) A_4 \\ H(n, \alpha, r) &= J_n(\gamma_s r) A_5 + Y_n(\gamma_s r) A_6 \end{aligned} \quad (3.6)$$

The spectral displacements are obtained from equations (3.5) and (3.6) as

$$\begin{aligned} u_r(n, \alpha, r) &= \gamma_1 J_n'(\gamma_1 r) A_1 + \gamma_1 Y_n'(\gamma_1 r) A_2 \\ &\quad + (n/r) J_n(\gamma_s r) A_3 + (n/r) Y_n(\gamma_s r) A_4 \\ &\quad - i \alpha \gamma_s J_n'(\gamma_s r) A_5 - i \alpha \gamma_s Y_n'(\gamma_s r) A_6 \\ u_\phi(n, \alpha, r) &= -(n/r) J_n(\gamma_1 r) A_1 - (n/r) Y_n(\gamma_1 r) A_2 \\ &\quad - \gamma_s J_n'(\gamma_s r) A_3 - \gamma_s Y_n'(\gamma_s r) A_4 \\ &\quad + (i \alpha n/r) J_n(\gamma_s r) A_5 + (i \alpha n/r) Y_n(\gamma_s r) A_6 \end{aligned} \quad (3.7)$$

$$u_z(n, \alpha, r) = i\alpha J_n(\gamma_1 r) A_1 + i\alpha Y_n(\gamma_1 r) A_2 \\ + (\alpha^2 - k_s^2) J_n(\gamma_s r) A_3 + (\alpha^2 - k_s^2) Y_n(\gamma_s r) A_6$$

The stress-displacement relations necessary for subsequent analysis are

$$\tau_{rr} = \lambda \operatorname{div} \underline{u} + 2\mu \partial u_r / \partial r \\ \tau_{r\phi} = \mu (\partial u_\phi / \partial r - (1/r) u_\phi + (1/r) \partial u_r / \partial \phi) \quad (3.8) \\ \tau_{rz} = \mu (\partial u_r / \partial z + \partial u_z / \partial r)$$

which can be represented spectrally, after simplifying by the use of the Bessel function differential equation

$$z^2 Z_n''(z) + z Z_n'(z) + (z^2 - n^2) Z_n(z) = 0,$$

as

$$\tau_{rr}(n, \alpha, r) = [2\mu \gamma_1^2 J_n''(\gamma_1 r) - \lambda k_1^2 J_n(\gamma_1 r)] A_1 \\ + [2\mu \gamma_1^2 Y_n''(\gamma_1 r) - \lambda k_1^2 Y_n(\gamma_1 r)] A_2 \\ + (2\mu n/r^2) [\gamma_s r J_n'(\gamma_s r) - J_n(\gamma_s r)] A_3 \\ + (2\mu n/r^2) [\gamma_s r Y_n'(\gamma_s r) - Y_n(\gamma_s r)] A_4 \\ - 2i\alpha \mu \gamma_s^2 J_n''(\gamma_s r) A_5 \\ - 2i\alpha \mu \gamma_s^2 Y_n''(\gamma_s r) A_6 \\ \tau_{r\phi}(n, \alpha, r) = (2n\mu/r^2) [-\gamma_1 r J_n'(\gamma_1 r) + J_n(\gamma_1 r)] A_1 \\ + (2n\mu/r^2) [-\gamma_1 r Y_n'(\gamma_1 r) + Y_n(\gamma_1 r)] A_2 \\ + (\mu/r^2) [2\gamma_s r J_n'(\gamma_s r) + (\gamma_s^2 r^2 - 2n^2) J_n(\gamma_s r)] A_3 \quad (3.9) \\ + (\mu/r^2) [2\gamma_s r Y_n'(\gamma_s r) + (\gamma_s^2 r^2 - 2n^2) Y_n(\gamma_s r)] A_4 \\ + (2i\alpha \mu n/r^2) [\gamma_s r J_n'(\gamma_s r) - J_n(\gamma_s r)] A_5 \\ + (2i\alpha \mu n/r^2) [\gamma_s r Y_n'(\gamma_s r) - Y_n(\gamma_s r)] A_6$$

$$\begin{aligned}
\tau_{rz}(n, \alpha, r) = & 2i\alpha\mu\gamma_1 J'_n(\gamma_1 r) A_1 \\
& + 2i\alpha\mu\gamma_1 Y'_n(\gamma_1 r) A_2 \\
& + (i\alpha\mu n/r) J_n(\gamma_s r) A_3 \\
& + (i\alpha\mu n/r) Y_n(\gamma_s r) A_4 \\
& + \mu\gamma_s (2\alpha^2 - k_s^2) J'_n(\gamma_s r) A_5 \\
& + \mu\gamma_s (2\alpha^2 - k_s^2) Y'_n(\gamma_s r) A_6
\end{aligned}$$

The boundary conditions

$$\begin{aligned}
\tau_{rr}(n, \alpha, b) &= \tau_{rr}^b \\
\tau_{r\phi}(n, \alpha, b) &= \tau_{r\phi}^b \\
\tau_{rz}(n, \alpha, b) &= \tau_{rz}^b \\
\tau_{rr}(n, \alpha, a) &= \tau_{rr}^a \\
\tau_{r\phi}(n, \alpha, a) &= \tau_{r\phi}^a \\
\tau_{rz}(n, \alpha, a) &= \tau_{rz}^a
\end{aligned}$$

yield the matrix equation

$$\begin{matrix} [P(n, \alpha)] & [A(n, \alpha)] & = & [\tau(n, \alpha)] \\ 6 \times 6 & 6 \times 1 & & 6 \times 1 \end{matrix} \quad (3.10)$$

and the spectral displacements equations (3.7) evaluated at $r=b$ and $r=a$ give the matrix equation

$$\begin{matrix} [R(n, \alpha)] & [A(n, \alpha)] & = & [u(n, \alpha)] \\ 6 \times 6 & 6 \times 1 & & 6 \times 1 \end{matrix} \quad (3.11)$$

The elements of the matrices $[P(n, \alpha)]$ and $[R(n, \alpha)]$ are given in Appendix A.

Equations (3.10) and (3.11) may be used to eliminate $[A(n, \alpha)]$ to give the formula

$$\begin{matrix} [P(n, \alpha)] & [R(n, \alpha)]^{-1} & [u(n, \alpha)] & = & [\tau(n, \alpha)] \\ 6 \times 6 & 6 \times 6 & 6 \times 1 & & 6 \times 1 \end{matrix} \quad (3.12)$$

which is of particular usefulness when analysing layered media by the finite element method [6].

4. INTERIOR AND EXTERIOR FLUIDS

(a) Interior Fluid

The linear acoustic equation [8]

$$\nabla^2 p_i = (1/c^2) \partial^2 p_i / \partial t^2 \quad (4.1)$$

is solved by replacing $p_i(r, \phi, z)$ by its Fourier transform representation and then integrating the resulting equation. Its spectral solution is

$$p_i(n, \alpha, r) = B_1 J_n(\gamma_i r) + B_2 Y_n(\gamma_i r) \quad (4.2)$$

The finiteness of $p_i(n, \alpha, r)$ at the origin $r=0$ requires B_2 to be set to zero. The relation between the fluid pressure and displacement, viz

$$\partial p_i / \partial r = \rho_i \omega^2 u_r \quad (4.3)$$

evaluated at the boundary $r=a$ enables the pressure to be expressed in terms of the boundary displacement $u_r(n, \alpha, a)$ as

$$p_i(n, \alpha, r) = \rho_i \omega^2 u_r(n, \alpha, a) J_n(\gamma_i r) / \gamma_i J_n'(\gamma_i a) \quad (4.4)$$

(b) Exterior Fluid

[8] The solution of the wave-equation relevant to outgoing waves is

$$p_e(n, \alpha, r) = B_3 H_n(\gamma_e r) \quad (4.5)$$

The boundary condition equation (4.3) evaluated at $r=b$ enables the pressure to be expressed in terms of the displacement $u_r(n, \alpha, b)$ as

$$p_e(n, \alpha, r) = \rho_e \omega^2 u_r(n, \alpha, b) H_n(\gamma_e r) / \gamma_e H_n'(\gamma_e b) \quad (4.6)$$

5. PIPE-FLUID BOUNDARY CONDITIONS

The boundary conditions to be applied at the interface between an elastic solid and an inviscid fluid are the continuity conditions of displacement and stress in the direction normal to the interface. The equations (4.4) and (4.6) reflect continuity of displacement and the continuity of normal stress in the absence of external forces on the

pipe's surfaces is given by the equation

$$\begin{bmatrix} P(n,\alpha) \\ 6 \times 6 \end{bmatrix} \begin{bmatrix} A(n,\alpha) \\ 6 \times 1 \end{bmatrix} = \begin{bmatrix} -p_e(n,\alpha,b), 0, 0, -p_i(n,\alpha,a), 0, 0 \\ 6 \times 1 \end{bmatrix}^T \quad (5.1)$$

which may be rearranged by making use of equations (4.4), (4.6) and (3.11) as

$$\begin{bmatrix} P(n,\alpha) + Q(n,\alpha) \\ 6 \times 6 \end{bmatrix} \begin{bmatrix} A(n,\alpha) \\ 6 \times 1 \end{bmatrix} = 0 \quad (5.2)$$

The elements of $[Q(n,\alpha)]$ are given in Appendix A.

The system of homogeneous linear equations (5.2) has a non-trivial solution only if the determinant of the coefficients vanishes. For given values of n and ω , there will be real and complex values of α at which the determinant vanishes. Plots of these values versus frequency are called wavenumber-frequency or dispersion plots. The real branches alone are of interest here; they are the wavenumbers at which free-waves propagate. The complex, or purely imaginary branches describe the evanescent waves whose effect decreases exponentially with distance. When an exterior fluid is present, there will be no real branches when $\alpha < k$ (except for pure torsion) due to energy loss in the form of acoustic radiation [8].

6. NUMERICAL RESULTS

Fortran programs have been written to compute and plot the real branches of the axial wavenumber versus frequency plots. A root is found simply by stepping through a range of α -values until a sign change occurs in the determinant: it is refined to a selected accuracy by repeated interval halving. Care must be taken with the Bessel function computations otherwise spurious roots may occur. Chosen SI constants are:

Steel: $E = 19.5E10$ $\sigma = 0.29$ $\rho = 7700.0$
 Water: $\rho = 1000.0$ $c = 1500.0$

Figure 2 shows the real branches of a water-filled pipe whose inner and outer radii are 0.2096m and 0.2350m respectively. The frequency range (2.8 times 'ring' frequency) and thickness to mean radius ratio (0.114) are sufficiently small enough to allow shell modes alone in the pipe's wall. The physical interpretation of the plots is discussed elsewhere [1]. The plots are compared with those obtained from a shell theory [3]. The significant differences at the higher frequencies occur when the waves are close to fluid-type waves; they are due to the assumption, in [3], that the fluid radius is equal to the mean radius of the shell.

Figure 3 shows wavenumber frequency plots of an in-vacuo pipe whose inner and outer radii are 0.10m and 0.20m respectively. The branches

labelled 4-10 involve 'thickness vibrations' of the pipe's wall. The plots for circumferential harmonics 1 and 2 are consistent with those obtained by Gazis [9] who discusses the nature of the wavenumber families. The plot for $n=0$ has many features in common with a plot obtained for a 0.10m thick plate that has zero wavenumber for the anti-plane strain branch - unpublished work arising from [6]. The curious behaviour of the branch labelled 6, for $n=0$ and 1, has not been adequately explained. It is also present in plate wavenumber plots.

7. ACKNOWLEDGEMENTS

Thanks are due to J H James for his helpful supervision of the project and its write-up, and also to E J Clement for his advice on the PDP-11/34 computer system.

S. A. Lester (Vacation Student
Mathematics Department
UMIST, Manchester)

SAL/jms

REFERENCES

1. FULLER, C.R. & FAHY, F.J., Characteristics of Wave Propagation and Energy Distribution in Cylindrical Elastic Shells Filled with Fluid, Institute of Sound and Vibration Research, Southampton, Contract Report No 81/10, March 1981.
2. WALTER, J.L., Coincidence of Higher Order Modes - a Mechanism of the Excitation of Cylindrical Shell Vibrations via Internal Sound, The Pennsylvania State University, PhD Thesis, 1979.
3. JAMES, J.H., Sound Radiation from Fluid-Filled Pipes, Admiralty Marine Technology Establishment, Teddington, AMTE(N) TM61048, September 1981.
4. LEISSA, A.W., Vibration of Shells, NASA SP-288, 1973.
5. KUMAR, R., Dispersion of Axially Symmetric Waves in Empty and Fluid-Filled Cylindrical Shells, Acustica 27(6), 1972, pages 318-329.
6. PESTELL, J.L. & JAMES, J.H., Sound Radiation from Layered Media, Admiralty Marine Technology Establishment, Teddington, AMTE(N) TM79423, October 1979.
7. MIKLOWITZ, J., The Theory of Elastic Waves and Waveguides, North-Holland, 1978.
8. JUNGER, M.C. & FEIT, D., Sound, Structures and their Interaction, MIT Press, 1972.
9. CAZIS, D.C., Three Dimensional Investigation of the Propagation of Waves in Hollow Circular Cylinders, J Acoust Soc Am, 31(5), 1959, pages 568-578.

A P P E N D I X A

The Matrix [P(n,α)]

$$P_{11} = 2\mu\gamma_1^2 J_n''(\gamma_1 b) - \lambda k_1^2 J_n(\gamma_1 b)$$

$$P_{12} = 2\mu\gamma_1^2 Y_n''(\gamma_1 b) - \lambda k_1^2 Y_n(\gamma_1 b)$$

$$P_{13} = (2\mu n/b^2)[\gamma_s b J_n'(\gamma_s b) - J_n(\gamma_s b)]$$

$$P_{14} = (2\mu n/b^2)[\gamma_s b Y_n'(\gamma_s b) - Y_n(\gamma_s b)]$$

$$P_{15} = -2i\alpha\mu\gamma_s^2 J_n''(\gamma_s b)$$

$$P_{16} = -2i\alpha\mu\gamma_s^2 Y_n''(\gamma_s b)$$

$$P_{21} = (2n\mu/b^2)[J_n(\gamma_1 b) - \gamma_1 b J_n'(\gamma_1 b)]$$

$$P_{22} = (2n\mu/b^2)[Y_n(\gamma_1 b) - \gamma_1 b Y_n'(\gamma_1 b)]$$

$$P_{23} = (\mu/b^2)[2\gamma_s b J_n'(\gamma_s b) + (\gamma_s^2 b^2 - 2n^2)J_n(\gamma_s b)]$$

$$P_{24} = (\mu/b^2)[2\gamma_s b Y_n'(\gamma_s b) + (\gamma_s^2 b^2 - 2n^2)Y_n(\gamma_s b)]$$

$$P_{25} = (2i\alpha\mu n/b^2)[b\gamma_s J_n'(\gamma_s b) - J_n(\gamma_s b)]$$

$$P_{26} = (2i\alpha\mu n/b^2)[b\gamma_s Y_n'(\gamma_s b) - Y_n(\gamma_s b)]$$

$$P_{31} = 2i\alpha\mu\gamma_1 J_n'(\gamma_1 b)$$

$$P_{32} = 2i\alpha\mu\gamma_1 Y_n'(\gamma_1 b)$$

$$P_{33} = (i\alpha n\mu/b)J_n(\gamma_s b)$$

$$P_{34} = (i\alpha n\mu/b)Y_n(\gamma_s b)$$

$$P_{35} = \mu\gamma_s(2\alpha^2 - k_s^2)J_n'(\gamma_s b)$$

$$P_{36} = \mu\gamma_s(2\alpha^2 - k_s^2)Y_n'(\gamma_s b)$$

The remaining rows, 4, 5 and 6, are obtained by setting $b=a$ in rows 1, 2 and 3.

The Matrix [R(n,a)]

$$\begin{aligned}
 r_{11} &= \gamma_1 J'_n(\gamma_1 b) & r_{12} &= \gamma_1 Y'_n(\gamma_1 b) \\
 r_{13} &= (n/b) J_n(\gamma_s b) & r_{14} &= (n/b) Y_n(\gamma_s b) \\
 r_{15} &= -i\alpha \gamma_s J'_n(\gamma_s b) & r_{16} &= -i\alpha \gamma_s Y'_n(\gamma_s b) \\
 r_{21} &= -(n/b) J_n(\gamma_1 b) & r_{22} &= -(n/b) Y_n(\gamma_1 b) \\
 r_{23} &= -\gamma_s J'_n(\gamma_s b) & r_{24} &= -\gamma_s Y'_n(\gamma_s b) \\
 r_{25} &= (i\alpha n/b) J_n(\gamma_s b) & r_{26} &= (i\alpha n/b) Y_n(\gamma_s b) \\
 r_{31} &= i\alpha J_n(\gamma_1 b) & r_{32} &= i\alpha Y_n(\gamma_1 b) \\
 r_{33} &= 0 & r_{34} &= 0 \\
 r_{35} &= (\alpha^2 - k_s^2) J_n(\gamma_s b) & r_{36} &= (\alpha^2 - k_s^2) Y_n(\gamma_s b)
 \end{aligned}$$

The remaining rows, 4, 5 and 6, are obtained by setting $b=a$ in rows 1, 2 and 3.

The Matrix [Q(n,a)]

The elements of [Q(n,a)] are identically zero, excepting the following

$$\begin{aligned}
 Q_{11} &= C_e r_{11} & Q_{12} &= C_e r_{12} & Q_{13} &= C_e r_{13} \\
 Q_{14} &= C_e r_{14} & Q_{15} &= C_e r_{15} & Q_{16} &= C_e r_{16} \\
 Q_{41} &= C_i r_{41} & Q_{42} &= C_i r_{42} & Q_{43} &= C_i r_{43} \\
 Q_{44} &= C_i r_{44} & Q_{45} &= C_i r_{45} & Q_{46} &= C_i r_{46}
 \end{aligned}$$

where

$$C_e = \rho_e \omega^2 H_n(\gamma_e b) / \gamma_e H'_n(\gamma_e b)$$

$$C_i = \rho_i \omega^2 J_n(\gamma_i a) / \gamma_i J'_n(\gamma_i a)$$

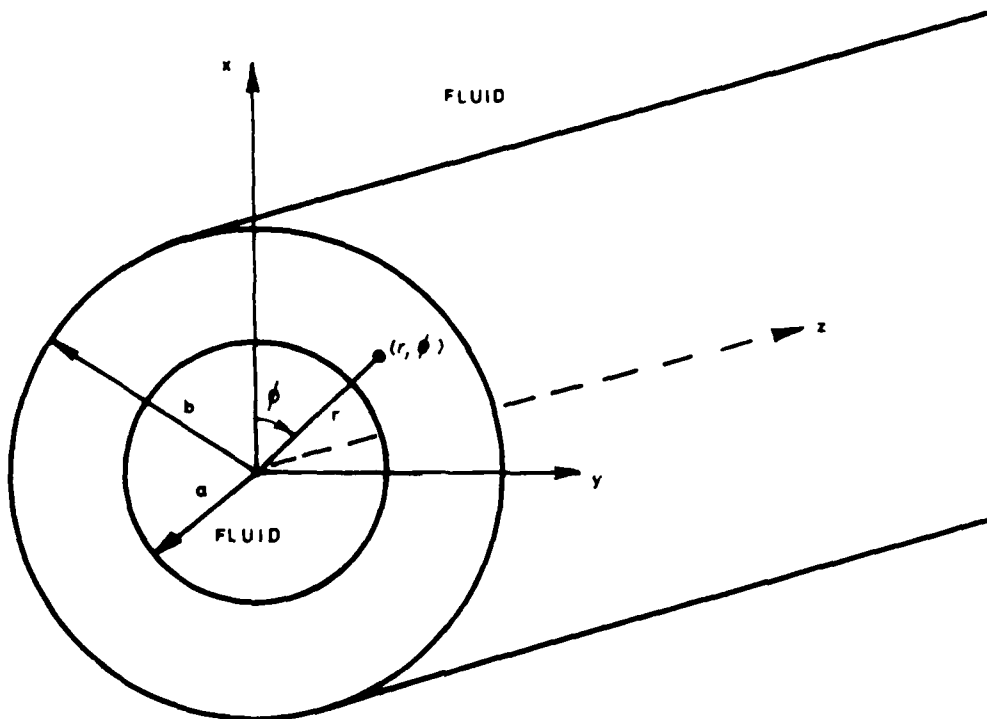


FIG. 1 SECTION THROUGH PIPE

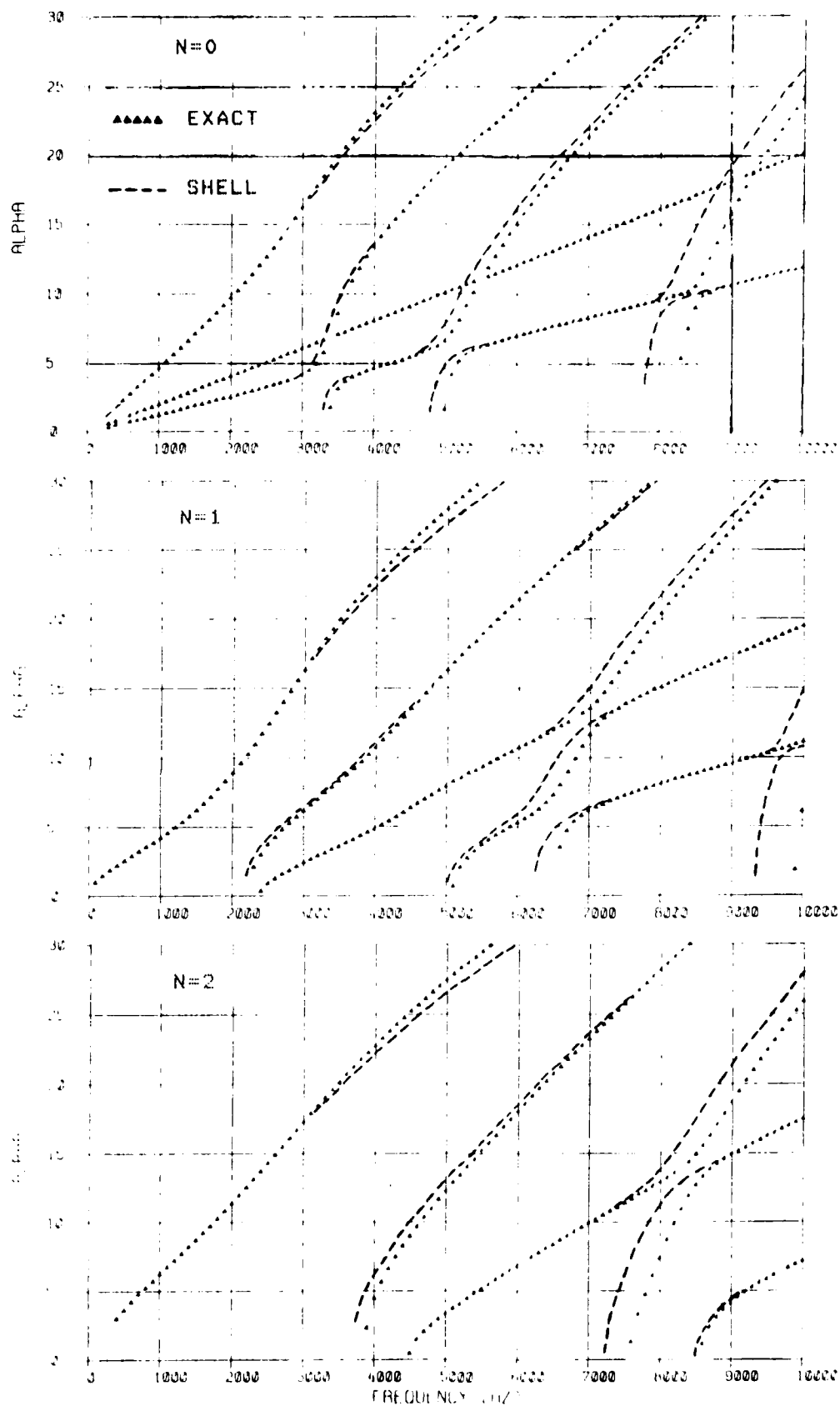


FIG. 2 AXIAL WAVENUMBER α , FREQUENCY PLOTS
WATER-FILLED STEEL PIPE, $A=0.2096\text{M}$, $B=0.2350\text{M}$.

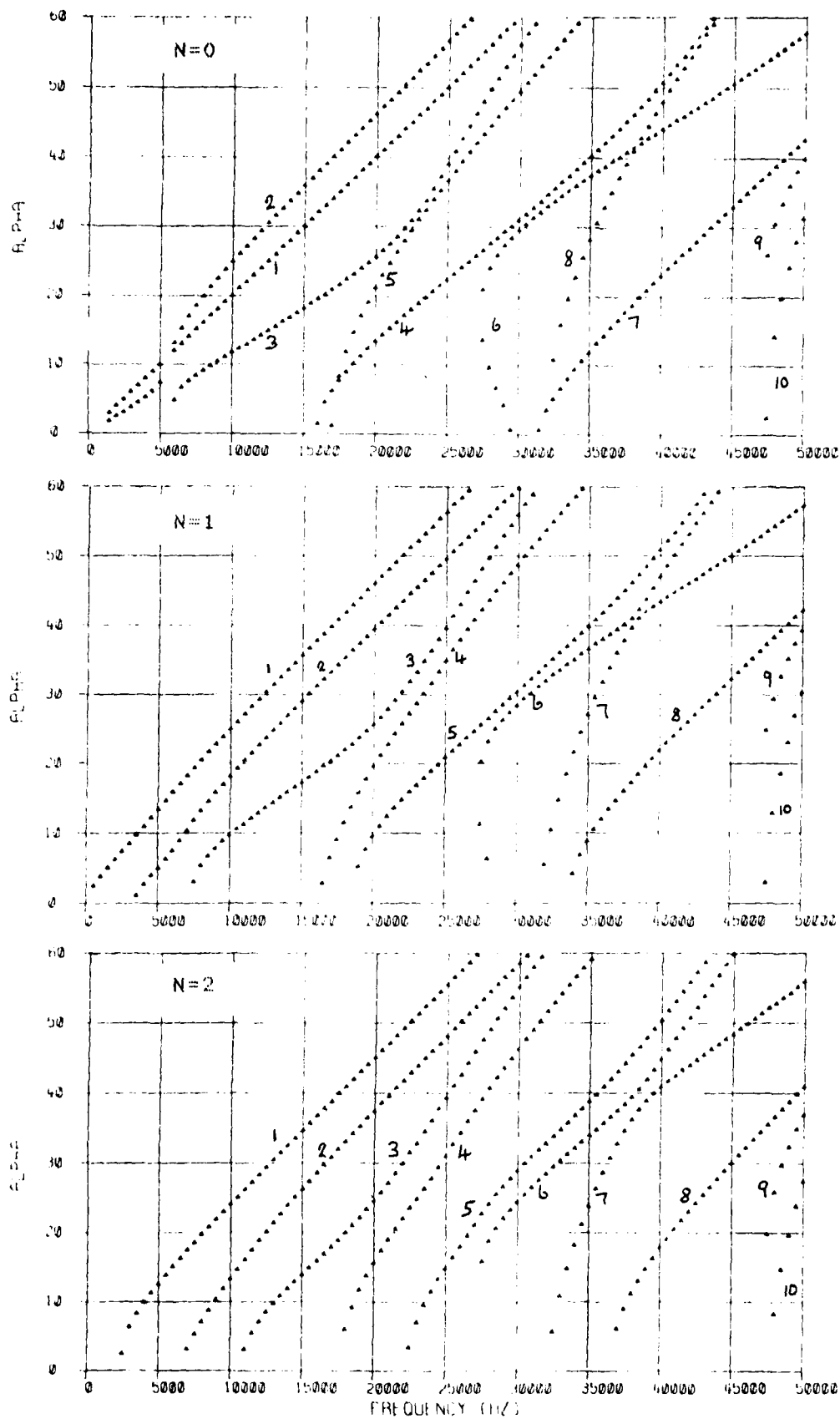


FIG. 3 AXIAL WAVENUMBER N . FREQUENCY PLOTS
STEEL PIPE, $A=0.10\text{M}$, $B=0.20\text{M}$.

DISTRIBUTION

	<u>Copy No</u>
DGRA/CS(RN)/DNOS	1
DAUWE (Dr I Roebuck)	2
DES Washington	3
CS(R) 2e (Navy)	4
DG Ships/DPT 17	5
DRIC	6-27
AMTE (Dunfermline)	28
AMTE (Teddington) File	29-36
AMTE (Teddington) Division N2 File	37-40

03-8
DTIC